

## Possible Phases and Some Properties of the One-Dimensional Metal with the Half-Filled Band

Minoru KIMURA

*Department of Physics, Kanazawa University, Kanazawa*

(Received August 17, 1974)

A one-dimensional metal with a half-filled band is studied by the model of Dzyaloshinskii and Larkin. The next-order renormalization group theory is applied. The invariant charges become smooth functions over all temperature. The possible phases—the singlet and the triplet Cooper pairing states, and SDW and CDW states at  $T \rightarrow 0$  are discussed. The criterion for these phases depends on the bare coupling constants via their signs and relative magnitudes. The phase diagram differs from that of the first-order theory. The Green's function, the vertex function, and  $2p_F$  and uniform response functions are found in the asymptotic power form. The exponents are universal except for the case of the repulsive couplings. The results are compared with the exact theorems about the Hubbard and Tomonaga models.

### § 1. Introduction

Theory of one-dimensional electron system has been a problem of much interest because of its amenability to exact treatment of the many body problem. Recently, however, interest has been renewed by experiments on 1-D conductors of many kinds.<sup>1)</sup> One of the most interesting features is the metal-insulator transition which takes place gradually at low temperatures. In addition, there have been observed evidences of a) the Peierls distortion in the conducting chains (Pt complexes<sup>2),3)</sup> and b) the continuous growing-up of the magnetic susceptibility at  $k=0$  and  $2p_F$  which is antiferromagnetic in character (TCNQ-NMP<sup>4),5)</sup>).

The property a) has been interpreted on the grounds of the  $2p_F$  soft-phonon mechanism.<sup>6),7)</sup> This seems to be qualitatively correct, but it should be remembered that a direct electron interaction would have also remarkable effect on the Peierls state.<sup>8)</sup> As for the property b), it is more evident that the electron interaction is mainly responsible. Indeed, one usually resorts to the Hubbard model with a half-filled band\*<sup>9)</sup> because the model seems appropriate for the  $\pi$ -electron system in the TCNQ salts.

The subject of the present paper has much bearing on this latter problem; the electrons in the 1-D half-filled band interacting via a potential of a finite range. We would like to study the problem in somewhat generalized situation, i.e., to include the arbitrariness in signs (attractive or repulsive) and the relative

\*<sup>9)</sup> References cited in Ref. 4). See also Ref. 24).

magnitudes of the couplings.

This model was first studied by Dzyaloshinskii and Larkin.<sup>9)</sup> They solved the problem involving three singular channels by means of a parquet method. They predicted thereby the ground state phases, namely, the normal, antiferromagnetic and singlet Cooper pairing (the last two could be accompanied with  $2p_F$  charge-density wave, so the Peierls state via the electron interaction by itself). However, the conclusion is not well reliable because they leave the destroying fluctuation effect peculiar in 1-D out of consideration.

Recently, the author,<sup>10)</sup> Menyhárd and Sólyom<sup>11)</sup> and Fukuyama et al.<sup>12)</sup> have investigated the similar model of Bychkov, Gor'kov and Dzyaloshinskii<sup>13)</sup> by the method of the renormalization group. M.S. showed the absence of any phase transitions at finite temperature and discussed the ground state phase by the next-order renormalization. Fukuyama et al. derived some physical properties on the same grounds, the results of which were comparable with the exact solutions.

This paper is devoted to a further study of D.L. model by the same method.<sup>14)</sup> The renormalizability of such a model has been demonstrated in the work.<sup>10), 12), 14)</sup> Actually, one could have easily anticipated from the very beginning that all the divergent graphs involved are exclusively of a logarithmic type in energy or temperature. This fascinating feature<sup>15)</sup> characteristic of the model makes the RG method greatly advantageous.

In § 2 the model and the prescription of RG are briefly reviewed. In § 3 we study the first order renormalization which reproduces D.L.'s results in a simple way.

In the next-order renormalization, which is the subject of §§ 4~6, it is shown that the fluctuating particle pairs play a crucial role to suppress the divergence in the invariant charges (IC) at all temperatures down to the absolute zero. This was just the case of M.S. Given the saturation values of IC at the Fermi level, it is easy to renormalize the various physical quantities. Thus, the asymptotic behavior of the Green's function and the vertex functions are found in the form of power.

In § 6 via the study of the critical fluctuations of the singlet and triplet Cooper pairings (SCP and TCP), spin density wave (SDW) and charge density wave (CDW) by Sólyom's method we propose the possible phase diagram versus  $\bar{g}_1$  and  $\bar{g}_4$ , which differs from that of D.L. in some regions. The critical exponents are universal except for the repulsive region (region I). The findings will have close correspondence to those of M.S. However, in what follows, particular emphasis will be made on the role played by the  $U$ -process which in almost all the cases of couplings strongly affects the physical properties of the system.

In § 7 we examine the static properties of the system. The magnetic susceptibility and the density response in the long wavelength limit are obtained in the form of power. In contrast to the critical responses studied in § 5 no divergent behavior is found up to the next-order renormalization, as should be

the case.

In § 8 some arguments are given for the interpretation and justification of the results.

§ 2. Hamiltonian and renormalization-group equations

Let us consider the 1-D model which is described by the Hamiltonian

$$H = \sum_{p, \alpha} \epsilon_p a_{p, \alpha}^+ a_{p, \alpha} + \frac{1}{2} \sum_{\langle p \rangle, \alpha, \beta} V(p_1, \dots, p_4) a_{p_1, \alpha}^+ a_{p_2, \beta}^+ a_{p_3, \alpha} a_{p_4, \beta} \cdot \delta_{p_1 + p_2, p_3 + p_4 + G}, \quad (2.1)$$

where  $G$  is 0 or the basic reciprocal lattice vector,  $\pm 4p_F$ .

Since the attention is focused on the “infrared singularity” at the Fermi level it is reasonable to assume as  $\epsilon_p = v(|p| - p_F)$  in general ( $v$  is the Fermi velocity), even for a tight binding electron. The potential  $V$  is assumed to act within a cutoff energy  $D \lesssim \epsilon_F$ , and depends on the character of the momentum transfer as

$$\begin{aligned} V(+ - - +) &= V(- + + -) = g_1 \text{ for the large momentum transfer } \sim 2p_F, \\ V(+ - + -) &= V(- + - +) = g_2 \text{ for the small momentum transfer } \ll p_F, \\ V(+ + - -) &= V(- - + +) = g_3 \text{ for the } U\text{-process,} \end{aligned} \quad (2.2)$$

where the sign  $+$  (or  $-$ ) restricts the range of corresponding argument  $p_i$  to be near  $+p_F$  (or  $-p_F$ ). The matrix elements of  $V$  other than (2.2) are assumed to be zero. For the following discussion the parameter  $g_4 = g_1 - 2g_2$  is also useful.

It is interesting to note that the model includes in itself the Tomonaga<sup>16)</sup> or the Luttinger<sup>17)</sup> model ( $g_1 = g_3 = 0$ ), the Hubbard model ( $g_1 = g_2 = g_3 \geq 0$ ) and the BGD model<sup>18)</sup> ( $g_3 = 0$ ).

Associated with the matrix elements (2.2), the vertex functions are written as

$$\Gamma(+ - - +) = g_1 \Gamma_1 \delta_{\alpha_1, \alpha_3} \delta_{\alpha_2, \alpha_4} - g_2 \Gamma_2 \delta_{\alpha_1, \alpha_4} \delta_{\alpha_2, \alpha_3}, \quad (2.3)$$

for the  $N$ -process, and

$$\Gamma(+ + - -) = g_3 \Gamma_3 (\delta_{\alpha_1, \alpha_3} \delta_{\alpha_2, \alpha_4} - \delta_{\alpha_1, \alpha_4} \delta_{\alpha_2, \alpha_3}), \quad (2.4)$$

for the  $U$ -process.

The scale-invariant charges (IC) for the problem are defined as

$$\Psi_i(x, u; g) = g_i d^2(x, u; g) \Gamma_i(x, u; g), \quad i = 1, 2, 3 \text{ or } 4, \quad (2.5)$$

where  $x$  and  $u$  are the characteristic energy and the cutoff of the interaction which are properly scaled, respectively, and  $g = (g_1, g_2, g_3)$ , and  $d(p)$  is defined through the full Green’s function by  $G(p) = d(p) G_0(p)$ .

Now, the scale invariance argument for  $\Psi$  leads to the Lie equations<sup>18)</sup>

$$x \frac{\partial}{\partial x} \Psi(x, u; g) = \frac{\partial}{\partial \xi} \Psi\left(\xi, \frac{u}{x}, \Psi(x, u; g)\right) \Bigg|_{\xi=1}, \quad (2.6)$$

with the boundary conditions

$$F(1, u; g) = 1, \text{ where } F=d \text{ or } \Gamma_i, \text{ hence } \Psi_i(1, u; g) = g_i. \quad (2.7)$$

In the same way we can derive for any renormalizable quantities  $A(x, u; g)$  the equation

$$x \frac{\partial}{\partial x} \ln A(x, u; g) = \frac{\partial}{\partial \xi} \ln A\left(x, \frac{u}{x}; \Psi(x, u; g)\right) \Big|_{\xi=1}, \quad (2.8)$$

which reflects the scale-transformation property of the function  $A$ .

Our problem is then primarily to solve Eq. (2.6). The right-hand side of (2.6), i.e., the input functions of the equations will be determined by means of the perturbation expansion in  $g$ . In practice, following the prescription of Eqs. (2.6) and (2.8) we should carry out the calculations only for the terms in the form of  $g^n \ln x$ . Once the invariant charges are known it is a matter of simple quadrature to obtain the function  $A$ .

### § 3. The first-order renormalization

Now, Let us begin with a brief study of the first-order renormalization. The first logarithmic terms arise from the second order diagrams. They are shown in Fig. 1, where the graphs a) and b) contribute to  $\Gamma_1$  and  $\Gamma_2$ , c) to  $\Gamma_2$  and d) and e) to  $\Gamma_3$ . Their perturbational expressions are summarized as

$$\begin{aligned} g_1 \Gamma_1^{(1)} &= g_1^2 \ln \frac{\epsilon}{2D}, & g_2 \Gamma_2^{(1)} &= \frac{1}{2} (g_1^2 - g_3^2) \ln \frac{\epsilon}{2D}, \\ g_3 \Gamma_3^{(1)} &= g_3 g_4 \ln \frac{\epsilon}{2D}, \end{aligned} \quad (3.1)$$

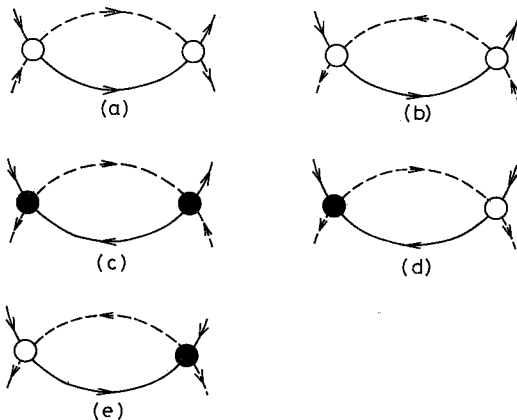


Fig. 1. The first-order graphs. The solid (broken) lines indicate the particles with the momentum  $\sim +(-)p_F$ . The white (black) circles denote the normal (Umklapp) scattering processes.

(in the unit  $1/\pi v = 1$ ) where  $\epsilon$  is the characteristic energy of the problem. The electron self-energy diagram does not contribute in this order, hence  $d=1$  and  $g_i \Gamma_i = \Psi_i$ .

If Eqs. (3.1) are used to obtain the first-order input functions we obtain the set of equations

$$\begin{aligned} x \frac{\partial}{\partial x} \Psi_1 &= \Psi_1^2, & x \frac{\partial}{\partial x} \Psi_4 &= \Psi_3^2, \\ x \frac{\partial}{\partial x} \Psi_3 &= \Psi_3 \Psi_4. \end{aligned} \quad (3.2)$$

These equations are exactly

analogous to those obtained by D.L. by the parquet-diagram method. We will not enter the detail of their solutions. Here, we only mention that they have led to the poles in  $\Psi$  and in the various responses at finite temperature characterized by

$$T_c \sim \begin{cases} D \exp(-1/|g_1|) & \text{for } g_1 < 0, \\ D \exp(-1/\sqrt{\gamma}) & \text{for } \gamma = g_3^2 - g_4^2 > 0. \end{cases} \quad (3.3)$$

At this point D.L. already emphasized that the singularities of this sort do not imply in any sense a finite-temperature phase transition, but it is only indicative of the fact that the problem tends to the strong coupling domain via  $T_c$ . Thus, we are forced to go beyond the first-order theory.

**§ 4. The next-order renormalization of the invariant charges**

The next-order logarithmic terms in the form of  $g^2 \ln x$  in IC arise from the “irreducible” diagrams for the vertex functions (Fig. 2) as well as for the self-energy function of the electron (Fig. 3). That the latter should be the case has been repeatedly stressed from the viewpoint of the consistency in the perturbation for many problems.<sup>19)</sup> The graphs in Figs. 2 and 3 involve the fluctuating electron-electron (hole-hole) pairs as well as electron-hole pairs. The former has been brought about by the inclusion of the  $U$ -process.

The perturbational expressions are obtained in a straightforward manner and summarized as

$$\begin{aligned} \Gamma_1^{(2)} &= \frac{1}{4} \{2g_2(g_1 - g_2) - g_3^2\} \ln \frac{\epsilon}{2D}, \\ \Gamma_2^{(2)} &= \frac{1}{4g_2} \{g_1^3 - 2g_1^2g_2 + 2g_1g_2^2 - 2g_2^3 + (g_2 - g_1)g_3^2\} \ln \frac{\epsilon}{2D}, \\ \Gamma_3^{(2)} &= -\frac{1}{4} (g_1^2 + 2g_1g_2 - 2g_2^2) \ln \frac{\epsilon}{2D} \end{aligned} \quad (4.1)$$

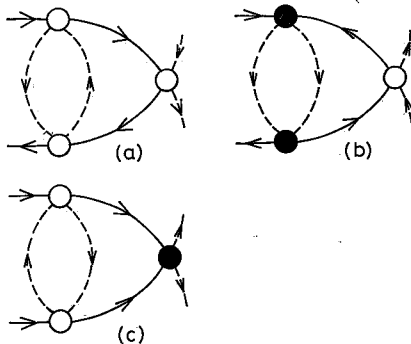


Fig. 2. The next-order graphs.

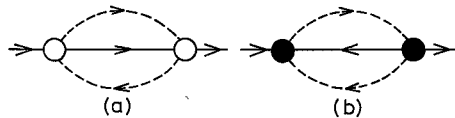


Fig. 3. The self-energy diagrams.

and

$$\Sigma(p) = \frac{1}{4} \left( g_1^2 + g_2^2 - g_1 g_2 + \frac{1}{2} g_3^2 \right) (\epsilon - \epsilon_p) \ln \frac{\epsilon}{2D}, \tag{4.2}$$

where  $\Gamma_1^{(2)}$  and  $\Gamma_2^{(2)}$  have come from the graphs (a) and (b) and  $\Gamma_3^{(2)}$  from (c).

Making use of Eqs. (4.1) and (4.2) together with (3.1) for the second-order input functions we are lead to the set of equations

$$x \frac{\partial}{\partial x} \Psi_1 = \Psi_1^2 + \frac{1}{2} \Psi_1^3, \tag{4.3a}$$

$$x \frac{\partial}{\partial x} \Psi_4 = \Psi_3^2 \left( 1 + \frac{1}{2} \Psi_4 \right), \tag{4.3b}$$

$$x \frac{\partial}{\partial x} \Psi_3 = \Psi_3 \Psi_4 \left( 1 + \frac{1}{4} \Psi_4 \right) + \frac{1}{4} \Psi_3^3. \tag{4.3c}$$

It is instructive to note in Eq. (4.3) the following obvious properties of  $\Psi$ :

- a)  $\Psi_1$  is definite in sign, and is always monotonic if  $g_1 \geq -2$ .
- b)  $\Psi_3$  is also definite but not always monotonic.
- c)  $\Psi_4$  is always monotonic provided  $g_3 \geq -2$ . If  $|g_4| \geq |g_3|$ , it is definite, but if  $|g_3| > |g_4|$ , it may pass through zero.

The solution of Eq. (4.3a) is written in the implicit form

$$\ln x = P_1(\Psi_1) - P_1(g_1), \tag{4.4}$$

where

$$P_1(\Psi) = \frac{1}{2} \ln \frac{\Psi + 2}{\Psi} - \frac{1}{\Psi}.$$

Equations (4.3b) and (4.3c) are integrated as follows:

i) for  $|g_3| \neq |g_4|$

$$\ln x = P_4(\Psi_4) - P_4(g_4), \quad \Psi_3^2 = \Psi_4^2 + 2C\Psi_4 + 4C, \tag{4.5}$$

where

$$P_4(\Psi) = \frac{1}{2} \left\{ \ln(\Psi + 2) - \frac{1}{2} \ln(\Psi^2 + 2C\Psi + 4C) + I(\Psi) \right\},$$

$$I(\Psi) = \frac{2-C}{2\sqrt{C(C-4)}} \ln \{ (\Psi + C - \sqrt{C(C-4)}) (\Psi + C + \sqrt{C(C-4)})^{-1} \}$$

and  $2C = (g_3^2 - g_4^2)/(g_4 + 2) = (\Psi_3^2 - \Psi_4^2)/(\Psi_4 + 2)$  is the first integral of Eq. (4.3b, c).

ii) for  $|g_3| = |g_4|$ , Eq. (4.5) reduces to

$$P_4(\Psi) = P_1(\Psi) \quad \text{and} \quad \Psi_3 = \pm \Psi_4, \tag{4.6}$$

iii) for  $g_3 = 0$ ,  $\Psi_3 = 0$  and  $\Psi_4 = g_4 = \text{const}$ , whereby the incommensurate case of

Menyhárd and Sólyom is recovered.

The behavior of these solutions is illustrated in Fig. 4.\*) We see at a glance that the solutions are regular over the whole range of the argument throughout all the case of the coupling parameters. At the same time it is apparent that Eq. (4.3) have the fixed points at  $x=0$ , where all the IC attain the saturation values. These are the outstanding features characteristic of the next-order renormalization. The limits of IC at  $x \rightarrow 0$  are easily evaluated by inspection of Eqs. (4.4) ~ (4.6) and summarized in Table I, where we have introduced for convenience the two parameters  $\bar{g}_1 = g_1/|g_s|$  and  $\bar{g}_4 = g_4/|g_s|$ .

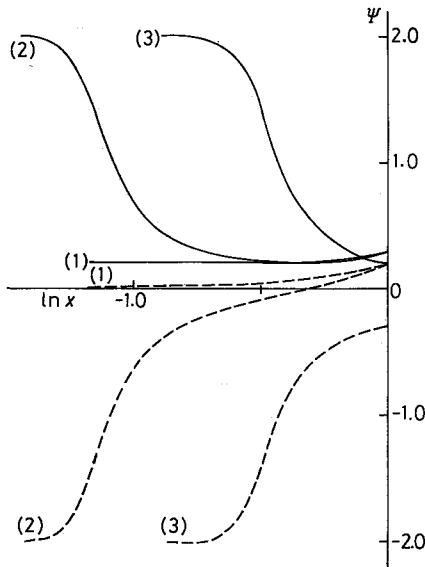


Table I. The saturation values of IC. The sign on  $\Psi_3$  coincides with that of  $g_3$ .  $\alpha = -C + \sqrt{C(4-C)}$ .

	I	II	III	IV
$\Psi_1(0)$	0	0	-2	-2
$\Psi_2(0)$	$-\alpha/2$	1	0	-1
$\Psi_3(0)$	0	$\pm 2$	$\pm 2$	0
$\Psi_4(0)$	$\alpha$	-2	-2	$\alpha$

I:  $\bar{g}_1 \geq 0, \bar{g}_4 \geq 1$ , II:  $\bar{g}_1 \geq 0, \bar{g}_4 < 1$ , III:  $\bar{g}_1 < 0, \bar{g}_4 < 1$ , IV:  $\bar{g}_1 < 0, \bar{g}_4 \geq 1$ . See Fig. 6.

Fig. 4. The numerical plots of the IC. The solid (broken) lines indicate  $\Psi_3$  ( $\Psi_4$ ).

### § 5. The next-order renormalization of the Green's function and the vertex functions

Now, we examine the Green's function and the vertex functions. With the help of Eqs. (4.1) and (4.2) the scale equations (2.8) for them lead to

$$\begin{aligned}
 x \frac{\partial}{\partial x} \ln \Gamma_1 &= \Psi_1 + \frac{1}{8} (\Psi_1^2 - \Psi_4^2 - 2\Psi_3^2), \\
 x \frac{\partial}{\partial x} \ln \Gamma_4 &= \frac{\Psi_4^2}{\Psi_4} - \frac{1}{8} (3\Psi_1^2 + \Psi_4^2 - 2\Psi_3^2),
 \end{aligned}
 \tag{5.1}$$

\*) The author appreciates Mr. M. Konishi's help in the numerical plots in Fig. 4.

$$\begin{aligned}
 x \frac{\partial}{\partial x} \ln \Gamma_3 &= \Psi_4 - \frac{1}{8} (3\Psi_1^2 - \Psi_4^2), \\
 x \frac{\partial}{\partial x} \ln d &= \frac{1}{16} (3\Psi_1^2 + \Psi_4^2 + 2\Psi_3^2).
 \end{aligned}
 \tag{5.2}$$

Here we have taken  $\Gamma_i$  as functions of a single variable characteristic of the problem, because it is in this form that they govern the various physical quantities in the logarithmic approximation.

The solutions of Eqs. (5.1) and (5.2) behave asymptotically in the form of power

$$d \approx (\epsilon/D)^\mu, \quad \Gamma_i \approx (\epsilon/D)^{\nu_i},
 \tag{5.3}$$

Table II. The exponents  $\mu$  and  $\nu_i$ .

	I	II	III	IV
$\mu$	$\alpha^2/16$	$3/4$	$3/2$	$3/4$
$\nu_{1,4}$	$-\alpha^2/8$	$-3/2$	$-3$	$-3/2$
$\nu_3$	$\alpha$	$-3/2$	$-3$	$-3/2$

where the conventional notations  $\epsilon$  and  $D$  have been restored. The exponents  $\mu$  and  $\nu_i$  are governed exclusively by the saturation values of IC, and estimated as shown in Table II. The numerical factors of the power are of magnitude  $O[1]$ , and are affected by the full

functional forms of IC. Here, no attempt was made to evaluate them precisely.

The form of  $d$  in Eq. (5.3) suggests an interesting property of the model: The original Fermi discontinuity is weakened drastically in the sense that the  $\delta(\epsilon)$  term at  $|p|=p_F$  in the spectral function  $\text{Im } G(\epsilon, p)$  smears out to the incoherent background, being replaced by a power form  $(\epsilon/D)^\mu$ . The reason is that  $d(\epsilon, p)$  in Eq. (5.3) depends on  $\epsilon$  and  $p$  only through an argument  $\epsilon \rightarrow \{\epsilon^2 - (vp)^2\}^{1/2}$ .\*) For the same reason the distribution function itself becomes continuous at the Fermi level with a trace of discontinuity left in the derivatives. Since Eq. (5.3) implies

$$dn_p/dp \propto \{(|p| - p_F)/D\}^{\mu-1},
 \tag{5.4}$$

the first derivative diverges at  $|p|=p_F$  in the region I, II and IV. In the region III the second derivative diverges. Note that the matter has been proved for the Tomonaga<sup>20)</sup> and the Luttinger<sup>17), 22)</sup> models and for the neutral Hubbard model.<sup>21), \*\*)</sup>

As mentioned in §1 the divergences in  $\Gamma_i$  taking place only at  $\epsilon=0$  imply that the phase transitions are possible to be manifested only at  $T=0\text{K}$ . This stands without violation of the theorem about the absence of any long-range

\*) See Ref. 26).

\*\*\*) Strictly speaking, the result does not agree with that for the Hubbard model<sup>6), 21)</sup> where a real gap opens up in the excitation spectrum. The situation gives us warning in applying the present scheme of renormalization since it would give rise to a power form singularity in general.



order in 1-D at finite  $T$ . Detailed discussion of the characters of the possible phases in the ground state is given in the next section.

§ 6. The critical fluctuations and the possible phases

Let us study the critical fluctuations of the order parameters which would specify the various phase transitions. The quantities which should be considered are defined by

$$\Pi^S(k, \omega) = -i \int dt e^{i\omega t} \sum_{p, p'} \langle T[a_{p, \uparrow}(t) a_{p'+k, \downarrow}(t) a_{p'+k, \downarrow}^+ a_{p, \uparrow}^+] \rangle, \tag{6.1a}$$

$$\Pi^T(k, \omega) = -i \int dt e^{i\omega t} \sum_{p, p'} \frac{p}{|p|} \langle T[a_{p, \uparrow}(t) a_{p+k, \uparrow}(t) a_{p'+k, \uparrow}^+ a_{p', \uparrow}^+] \rangle \frac{p'}{|p'|}, \tag{6.1b}$$

$$\chi(k, \omega) = -i \int dt e^{i\omega t} \sum_{p, p'} \langle T[a_{p, \uparrow}^+(t) a_{p+k, \downarrow}(t) a_{p'+k, \downarrow}^+ a_{p', \uparrow}] \rangle, \tag{6.1c}$$

$$N(k, \omega) = -i \int dt e^{i\omega t} \sum_{\substack{p, p' \\ \alpha, \beta}} \langle T[a_{p, \alpha}^+(t) a_{p+k, \alpha}(t) a_{p'+k, \beta}^+ a_{p', \beta}] \rangle, \tag{6.1d}$$

with  $k \approx 2p_F$ . Solyom suggested, however, none of these functions are the proper quantities satisfying the renormalizability condition. He introduced the auxiliary renormalizable functions defined by

$$\bar{F}_i = \frac{\partial F_i}{\partial \ln x}, \quad \text{where } F_i = \Pi^S, \Pi^T, \chi \text{ or } N, \tag{6.2}$$

where  $x$  is the characteristic energy properly scaled as before.

To understand why (6.2) is the proper function we recall that D.L. started, alternatively, with the three-pole external vertices each of which is certainly renormalizable. The differentiation in (6.2) indicates cutting of any singular pair lines in the graphs for the functions  $F$ , thus leading to the squared three-pole

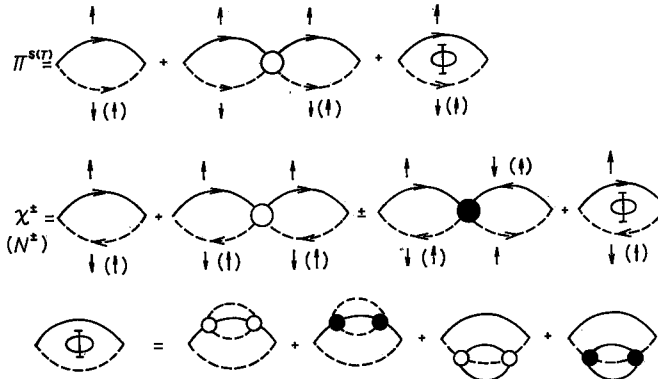


Fig. 5. The diagram expansions for the critical fluctuations.

vertices.

The graphical expansion for each  $F_i$  is shown in Fig. 5. To be consistent with the foregoing approximation we take account of the leading logarithms up to the next order.

Because the  $U$ -process is involved directly in the graphs of SDW and CDW we have to consider, not only  $+2p_F$  to  $+2p_F$  but also  $+2p_F$  to  $-2p_F$  responses for each of them. For convenience, we introduce the two modes

$$\chi^\pm = \chi_{++} \pm \chi_{+-}, \tag{6.3}$$

and similarly,  $N^\pm$ .

Simple calculations yield the perturbational expressions

$$\begin{aligned} \bar{\Pi}^s(\omega) &= \ln \frac{\omega}{2D} \left[ 1 + \frac{1}{2} \{g_1 + g_2 + \emptyset(g)\} \ln \frac{\omega}{2D} + \dots \right], \\ \bar{\Pi}^r(\omega) &= \ln \frac{\omega}{2D} \left[ 1 + \frac{1}{2} \{g_2 - g_1 + \emptyset(g)\} \ln \frac{\omega}{2D} + \dots \right], \\ \bar{\chi}^\pm(\omega) &= \frac{1}{2} \ln \frac{\omega}{2D} \left[ 1 + \frac{1}{2} \{-g_2 \mp g_3 + \emptyset(g)\} \ln \frac{\omega}{2D} + \dots \right], \\ \bar{N}^\pm(\omega) &= \ln \frac{\omega}{2D} \left[ 1 + \frac{1}{2} \{2g_1 - g_2 \pm g_3 + \emptyset(g)\} \ln \frac{\omega}{2D} + \dots \right], \end{aligned} \tag{6.4}$$

where

$$\emptyset(g) = \frac{1}{2} (g_1^2 + g_2^2 - g_1 g_2 + \frac{1}{2} g_3^2). \tag{6.5}$$

By Eq. (6.4) the scale equations (2.8) for each  $F$  lead to

$$x \frac{\partial \ln \bar{\Pi}^s}{\partial x} = \Psi_1 + \Psi_2 + \emptyset(\Psi), \tag{6.6a}$$

$$x \frac{\partial \ln \bar{\Pi}^r}{\partial x} = \Psi_2 - \Psi_1 + \emptyset(\Psi), \tag{6.6b}$$

$$x \frac{\partial \ln \bar{\chi}^\pm}{\partial x} = -\Psi_2 \mp \Psi_3 + \emptyset(\Psi), \tag{6.6c}$$

$$x \frac{\partial \ln \bar{N}^\pm}{\partial x} = 2\Psi_1 - \Psi_2 \pm \Psi_3 + \emptyset(\Psi), \tag{6.6d}$$

from which the asymptotic expressions are obtained as

$$F_i(\omega) \propto \bar{F}_i(\omega) \propto (\omega/D)^{\alpha_i}. \tag{6.7}$$

The critical exponents  $\alpha_i$  are easily evaluated by the saturation values of IC and summarized in Table III, where in order to make the contrast clear the S6lyom's case ( $g_3=0$ ) is tabulated together.

Table III. The critical exponents  $\alpha_i$ .

	I	II	III	IV	V	VI
$\Pi^s$	$-\alpha/2$	$5/2$	$1$	$-3/2$	$-g_4/2$	$-3/2$
$\Pi^r$	$-\alpha/2$	$5/2$	$5$	$5/2$	$-g_4/2$	$5/2$
$\chi^*$	$\alpha$	$-3/2^*$	$1^*$	$5/2$	$g_4/2$	$5/2$
$N^\pm$	$\alpha$	$5/2^*$	$5^*$			
		$5/2^*$	$1^*$	$-3/2$	$g_4/2$	$-3/2$
		$-3/2^*$	$-3^*$			

V:  $g_3=0, g_1 \geq 0$ , VI:  $g_3=0, g_1 < 0$ .

\*: For  $g_3 > 0$ . For  $g_3 < 0$  the upper and the lower numbers are interchanged.

By the definition (6.3) the divergence in  $\chi$  (and in  $N$ ) may be brought about from either of  $\chi^+(N^+)$  or  $\chi^-(N^-)$ , therefore it depends on  $g_3$  only via its absolute value. Bearing this in mind we can obtain at once the selection rule for the possible phases at  $T \rightarrow 0K$ . The phase diagram versus  $\bar{g}_1$  and  $\bar{g}_4$  is shown in Fig. 6, where the boundaries between the phases belong to the shaded sides, respectively.\*)

In comparing these results with those for  $g_3=0$  (cf. S6lyom) it becomes clear that the  $U$ -process makes marked influences on the properties of the system. In particular, we should note the following points:

- In the region III, only CDW diverges for  $g_3 \neq 0$ , while for  $g_3=0$  both CDW and SCP do.
- In the region II, although SDW and CDW diverges for both cases, their exponents are greatly enhanced for the case  $g_3 \neq 0$ . Such an instability enhancement in the commensurate case should have been anticipated.
- The region I is not so altered in quality, but the numerical differences in the exponents are found between both cases.

In view of the situation C) it is possible to expect that all the predictions made about the Tomonaga<sup>20)</sup> or the Luttinger<sup>22)</sup> model can still apply qualitatively in the region I even if  $g_3 \neq 0$ , but no longer stand in the regions II~IV.

Finally, it is worth while to comment on SCP and TCP in the region I. Here, the

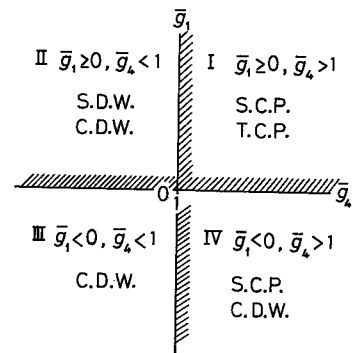


Fig. 6. The phase diagram versus  $\bar{g}_1$  and  $\bar{g}_4$ .

\*) The situation of the phase diagram being scaled by  $|g_3|$  is a consequence of the result that the saturation values of IC are determined through the sign of the first integral C (see § 4 and Table I). This feature is already marked in the first order theory where the first integral is given by  $\gamma = \Psi_3^2 - \Psi_4^2$ .

first order theory is reliable. If the solutions of Eq. (3.2) for  $\bar{g}_1 \geq 0$  and  $\bar{g}_4 \geq 1$  are substituted into Eq. (6.6a, b) we obtain a more detailed expression for Eq. (6.7)

$$\bar{\Pi}^S(\omega) = \left(1 - g_1 \ln \frac{\omega}{2D}\right)^{-3/2} \Pi(\omega), \tag{6.8}$$

$$\bar{\Pi}^T(\omega) = \left(1 - g_1 \ln \frac{\omega}{2D}\right)^{1/2} \Pi(\omega), \tag{6.9}$$

where

$$\Pi(\omega) = \left\{ \text{sh} \left( g' \ln \frac{\omega}{2D} + \delta \right) / \text{sh} \delta \right\}^{1/2}, \quad \delta = -\text{cth}^{-1}(g_4/g')$$

and  $g' = (g_4^2 - g_3^2)^{1/2}$ . We see that TCP is more strongly divergent than SCP. Equations (6.8) and (6.9) are a natural extension of the result in Ref. 12).

### § 7. Uniform susceptibilities

In this section we study some static properties, namely, the paramagnetic susceptibility, density response and the diamagnetic current response in the long wavelength limit by following the work of Fukuyama et al.

The magnetic susceptibility  $\chi$  and density response  $N$  are defined by (6.1c, d), respectively, but in the neighborhood of  $k \sim 0$  and  $\omega/k \rightarrow 0$  (the so-called  $k$ -limit). The current response is defined by

$$Q(k, \omega) = -i \int dt e^{i\omega t} \sum_{\substack{p, p' \\ \alpha, \beta}} p \langle T [a_{p, \alpha}^+(t) a_{p+k, \alpha}(t) a_{p'+k, \beta}^+ a_{p', \beta}] \rangle p'. \tag{7.1}$$

The first logarithmic corrections of these quantities arise in the second order perturbation. The graphs are shown in Fig. 7 schematically. In order to include the  $U$ -process the new Umklapp graphs are added to the normal graphs as shown in Fig. 8.

First consider the magnetic susceptibility. The graph (b) is identically zero

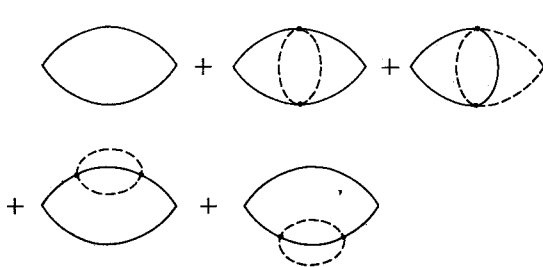


Fig. 7. The diagram expansions for the uniform susceptibilities.

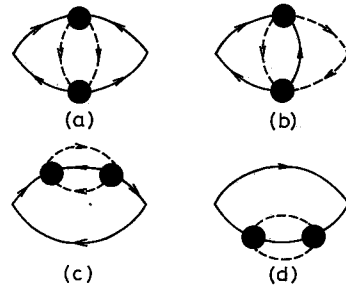


Fig. 8. The Umklapp graphs for the uniform susceptibilities.

because of the cancellation in summing up the spin directions. The graph (a) is compensated out to zero by the graph (c) + (d). Therefore no divergent correction arises from the  $U$ -graphs.

Next, in the density and current responses all the  $N$ -graphs have been cancelled out to zero in accord with the Ward identity requirement.<sup>12)</sup> As for the current response, in particular, the same type of cancellation also occurs on the  $U$ -graphs, i.e., the sum (a) + (b) compensates exactly the sum (c) + (d).

Turning to the density response we find that such a full cancellation does not take place. The perturbational calculations for the graphs (a) ~ (d) give

$$N^{(2)}(k, 0) = \frac{1}{4} N_0 g_s^2 \ln \frac{vk}{2D}. \quad (7.2)$$

The scale equation (2.8) for it becomes

$$x \frac{\partial \ln(N/N_0)}{\partial x} = \frac{1}{4} \Psi_s^2, \quad (7.3)$$

from which the asymptotic solution for  $N$  is obtained as

$$N(k, 0)/N_0 = (vk/D)^{\Psi_s^2(0)/4}. \quad (7.4)$$

Summarizing the arguments we arrive at the conclusion:

A) The magnetic susceptibility is the same as that for the incommensurate case,  $g_s=0$ . Therefore, the result in Ref. 12) is carried over:  $\chi$  reduces to the finite  $\chi(0, 0) = \chi_0$  for  $g_1 \geq 0$  and tends to zero in such a way as  $\sim (vk/D)^2$  for  $g_1 < 0$ . We note that this is in good accord with the exact result for the repulsive and attractive Hubbard models.<sup>23), 24)</sup>

B) The current response does not undergo any divergent correction.

C) The density response is renormalized by the  $U$ -graphs alone. It reduces to the finite  $N(0, 0) = N_0$  for  $\bar{g}_4 \geq 1$ . Again, this is in accord with the result for the Tomonaga model<sup>17)</sup> where it was proved that any singular change in  $N(k \sim 0)$  does not occur as long as the coupling is weak ( $|g_2| < 1$ ). If  $\bar{g}_4 < 1$ , on the other hand,  $N(k \sim 0)$  is renormalized to zero in such a way as  $\sim vk/D$ . The non-zero value of  $\Psi_s(0)$  gives rise to this remarkable change.

## § 8. Conclusion

There is a fundamental difference between 3-D and 1-D systems. In the perturbational point of view, this difference manifests itself already in the first-order theory, but in a more profound way in the next-order theory: The fluctuations destroy the long-range orders and lower the critical temperature down to 0K. This is the physical ground of the well-known theorem about the absence of long-range orders at  $T > 0$ K in 1-D and has been taken into account throughout this paper.

However, one might object to the validity of the next-order renormalization

because the present IC attain the values of  $O[1]$  except for the region I. In this sense, the strong coupling domain characterized by (3.3) persists even in the next-order theory.

Another serious question for the present results would arise from consistency arguments. Nagaoka<sup>20)</sup> comments on the possible (co)existence of CDW or (and) SCP in the attractive Hubbard model (in the region IV) which should correspond to only SDW in the repulsive Hubbard model (in the region II). From this viewpoint it is difficult to understand the coexistence of CDW divergence in the region II. This problem would not be solved within the framework of the present approximation.

Nevertheless, many of the results are qualitatively correct as compared with the exact solutions for some particular cases, as mentioned in the preceding sections. Thus we expect the theory to be applicable also to the problem of the dynamical scaling of the model.<sup>20)</sup>

Finally, we note that the specific heat which has been suggested to be linear in temperature for the Hubbard model<sup>24)</sup> and the BGD model<sup>25)</sup> is so general that it must be kept for the present model in all the cases of the couplings.

### Acknowledgements

The author would like to express his thanks to Professr S. Nakajima, Dr. Y. Kurihara and Dr. Y. Kuroda for their valuable discussions and supports in the work and to Professor A. Yoshimori and Professor Y. Nagaoka for giving him valuable comments. He is also grateful to Professor H. Fukuyama for his valuable discussions to which the work is much indebted.

### References

- 1) I. F. Shchegolev, *Phys. Stat. Sol. a* **12** (1972), 9.
- 2) B. Renker, H. Rietschel, L. Pintshovius, W. Gläser, B. Renker and D. Kuse and M. J. Rice, *Phys. Rev. Letters* **30** (1973), 1144.
- 3) R. Comés, M. Lambert and H. Launois, *Phys. Rev.* **B8** (1973), 571.
- 4) A. J. Epstein, S. Etemad, A. F. Garito and A. J. Heeger, *Phys. Rev.* **B5** (1972), 952.
- 5) E. Ehrenfreund, E. F. Rybaczewskii, A. F. Garito and A. J. Heeger, *Phys. Rev. Letters* **28** (1972), 873.
- 6) M. J. Rice and S. Strässler, *Solid State Comm.* **13** (1973), 125, 697.
- 7) B. R. Patten and L. J. Sham, *Phys. Rev. Letters* **31** (1973), 631.
- 8) A. A. Obchinnikov, I. I. Ukrainskii and G. F. Wentzel, *Uspekhi Fiz. Nauk SSSR* **108** (1972), 81.
- 9) I. Ye. Dzyaloshinskii and A. I. Larkin, *Zhur. Eksp. i Teor. Fiz.* **61** (1971), 791.
- 10) M. Kimura, *Prog. Theor. Phys.* **49** (1973), 697.
- 11) N. Menyhárd and Sóllyom, *J. Low Temp. Phys.* **12** (1973), 529.  
J. Sóllyom, *J. Low Temp. Phys.* **12** (1973), 547.
- 12) H. Fukuyama, T. M. Rice, C. M. Varma and B. I. Halperin, *Phys. Rev.* **B5** (1974), 3775.
- 13) Yu. A. Bychkov, L. P. Gor'kov and I. Ye. Dzyaloshinskii, *Zhur. Eksp. i Teor. Fiz.* **50** (1966), 783.

- 14) Preliminary works have been reported by; M. Kimura, *Sci. Rep. Kanazawa univ.* **18** (1973), 55; M. Konishi and M. Kimura *Prog. Theor. Phys.* **52** (1974), 353. Some errors in the latter work is corrected in the present paper.
- 15) A. A. Abrikosov and A. A. Migdal, *J. Low Temp. Phys.* **3** (1970), 519.
- 16) S. Tomonaga, *Prog. Theor. Phys.* **5** (1950), 544.
- 17) D. C. Mattis and E. H. Lieb, *J. Math. Phys.* **6** (1965), 304.
- 18) N. N. Bogoliubov and D. N. Shirkov, *Introduction to the Theory of Quantized Fields* (Interscience Publishers, INC., New York, 1956).
- 19) B. Roulet, J. Gavoret and P. Nozierés, *Phys. Rev.* **178** (1969), 1084.
- 20) H. Gutfreund and M. Schick, *Phys. Rev.* **168** (1968), 418.
- 21) E. H. Lieb and F. Y. Wu, *Phys. Rev. Letters* **20** (1968), 1445.
- 22) A. Luther and I. Peshel, *Phys. Rev. Letters* **32** (1974), 992; *Phys. Rev.* **B9** (1974), 2911.
- 23) M. Takahashi, *Prog. Theor. Phys.* **42** (1969), 1098; **43** (1970), 1619.
- 24) H. Shiba, *Prog. Theor. Phys.* **48** (1972), 2171.
- 25) Y. Nagaoka, *Prog. Theor. Phys.* **52** (1974), 1716.
- 26) H. Fukuyama and M. Kimura, to be published.